Title
A Stable Silanol Triad in the Zeolite Catalyst SSZ-70

Journal
Angewandte Chemie International Edition, 59(27)

ISSN
1433-7851

Authors
Schroeder, Christian
Mück-Lichtenfeld, Christian
Xu, Le
et al.

Publication Date
2020-06-26

DOI
10.1002/anie.202001364

Peer reviewed

How to cite: *Angew. Chem. Int. Ed.* **2020**, *59*, 10939–10943
International Edition: doi.org/10.1002/anie.202001364
German Edition: doi.org/10.1002/ange.202001364

Zeolites

A Stable Silanol Triad in the Zeolite Catalyst SSZ-70

Christian Schroeder, Christian Mück-Lichtenfeld, Le Xu, Nicolás A. Grosso-Giordano, Alexander Okrut, Cong-Yan Chen, Stacey I. Zones, Alexander Katz,* Michael Ryan Hansen, and Hubert Koller**

Abstract: *Nests of three silanol groups are located on the internal pore surface of calcined zeolite SSZ-70. 2D ^{1}H double/triple-quantum single-quantum correlation NMR experiments enable a rigorous identification of these silanol triad nests. They reveal a close proximity to the structure directing agent (SDA), that is, N,N′-diisobutyl imidazolium cations, in the as-synthesized material, in which the defects are negatively charged (silanol dyad plus one charged SiO^- siloxy group) for charge balance. It is inferred that ring strain prevents the condensation of silanol groups upon calcination and removal of the SDA to avoid energetically unfavorable three-rings. In contrast, tetrad nests, created by boron extraction from B-SSZ-70 at various other locations, are not stable and silanol condensation occurs. Infrared spectroscopic investigations of adsorbed pyridine indicate an enhanced acidity of the silanol triads, suggesting important implications in catalysis.*

Zeolites are microporous materials comprising a 3D $TO_{4/2}$ network of tetrahedral framework atoms (T = Si, Al, Ti, B, …). They are essential in numerous commercial applications, such as acid catalysis and redox chemistry.[1] One of the main reasons for their high catalytic selectivity is that zeolites offer unique reaction spaces in their micropores, which control the reaction mechanism by adsorption effects. Silanol defects contribute to the hydrophilic properties and thus influence adsorption in these zeolite pores,[2] but they can also be an integral part of the reaction center, such as for the Beckmann rearrangement of cyclohexanone oxime to ε-caprolactame in ZSM-5 or Beta zeolites.[3] More recently, silanol groups were reported to contribute to oxidation catalysis, through cooperativity with Lewis acid sites.[4] These effects include olefin epoxidation reactions in titanosilicates synthesized from SSZ-70 precursors.[5]

There has been a longstanding debate in the literature regarding the nature of defect sites and their formation in zeolites.[6] The removal of a T atom was suggested to create a so-called silanol nest. However, this extraction typically requires acid treatment or steaming at elevated temperatures, resulting in condensation and hydrolysis reactions (migration of vacancies).[7] Thus, such vacancies assemble in larger entities, either forming internal mesopores or disappearing on the crystal surface. Therefore, the stability of the postulated SiOH tetrad nests was subject to critical scrutiny.[6e,8] Clearly, so far, investigations lacked the methodology to rigorously determine the number of silanol groups in a defect site.

Herein we utilize double (or higher multi) quantum ^{1}H MAS NMR experiments (MAS = magic angle spinning) to measure homonuclear dipolar interactions.[9] We have previously applied such methods to investigate defect sites in as-made zeolites,[10] as well as Brønsted acid sites in zeolite Y.[11] The ^{1}H dipolar interactions directly probe the spatial proximities of silanol groups, enabling their cluster sizes to be determined within a distance range of typically 5 Å (to a maximum of 8 Å).

Zeolite SSZ-70[12] (framework type code: *-SVY)[13] is related to zeolite ITQ-1[14] (MWW), which both consist of the same type of layers, Figure 1. SSZ-70 is a partially disordered material due to disorder in the layer stacking. While these layers are fully interconnected in ITQ-1 (Figure 1b), they are shifted in SSZ-70, resulting in structural Q^3 groups with dangling silanols (Figure 1a,c). Additionally, the atomic positions of Si and O atoms in these Q^3 groups were refined with only 50% occupancy in the Rietfeld analysis. Therefore, SiOH triad nests (Figure 1c) were proposed, while hydrogen atoms could not be located.[12]

The ^{29}Si MAS NMR spectra of SSZ-70 (Figure S1a in the Supporting Information and Refs. [12,15]) and ITQ-1[14] are almost identical, except for the presence of Q^3 defect sites in SSZ-70 that do not exist in ITQ-1. This similarity manifests that the layers are topologically identical in both zeolites. However, the two materials exhibit distinct defect site

[*] C. Schroeder, Prof. M. R. Hansen, Dr. H. Koller
Institut für Physikalische Chemie
Westfälische Wilhelms-Universität
Corrensstrasse 28/30, 48149 Münster (Germany)
E-mail: hubert.koller@uni-muenster.de
C. Schroeder, Dr. H. Koller
Center of Soft Nanoscience, Westfälische Wilhelms-Universität
Busso-Peus-Strasse 10, 48149 Münster (Germany)
Dr. C. Mück-Lichtenfeld
Organisch-Chemisches Institut, Westfälische Wilhelms-Universität
Corrensstrasse 40, 48149 Münster (Germany)
Dr. L. Xu, Dr. N. A. Grosso-Giordano, Dr. A. Okrut, Prof. A. Katz
Department of Chemical and Biomolecular Engineering
University of California
Berkeley, CA 94720 (USA)
E-mail: askatz@berkeley.edu
Dr. C.-Y. Chen, Dr. S. I. Zones
Chevron Energy Technology Company
Richmond, CA 94804 (USA)
E-mail: SIZO@chevron.com
Supporting information and the ORCID identification number(s) for the author(s) of this article can be found under: https://doi.org/10.1002/anie.202001364.

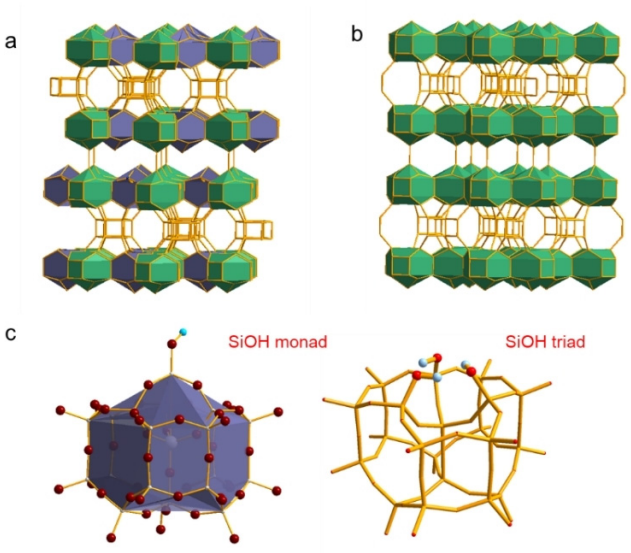

Figure 1. a) Framework topology of zeolite SSZ-70, highlighting in different colors the cages, which are interconnected (green) or having silanol groups (blue), b) framework topology of ITQ-1 with all cages interconnected, c) silanol monad and triad model; cyan H, red O. O atoms are omitted in models in (a) and (b).

properties, as unveiled by the ^{1}H double-quantum single-quantum (DQ-SQ) correlation NMR spectra of SSZ-70 (Figure 2a) and ITQ-1 (Figure 2b), displaying clear differences in the silanol pairing pattern. These 2D experiments show in the SQ dimension the chemical shifts of the two protons that are in spatial proximity and the sum of their two chemical shifts is shown on the DQ axis.

Analysis of 1D slices (Figure S3) taken from the 2D data of calcined SSZ-70 (Figure 2a) shows three major cross-correlation signals at DQ chemical shifts of 7.3 ppm (3.1 + 4.2), 8.6 ppm (3.1 + 5.5), and 9.7 ppm (4.2 + 5.5). The combination of these three cross-correlations is due to the triplet of SiOH groups in mutual spatial proximity (Figure 1c). Some minor auto-correlation intensity at SQ chemical shifts of approximately 1–3 ppm are assigned to randomly paired silanols at internal or external surface sites, and an autocorrelation at 4.3 ppm is due to physisorbed water and/or hydrogen-bonded silanol pairs at other positions. In contrast, ITQ-1 only shows three auto-correlation signals with SQ chemical shifts of 1.0, 1.3, and 2.1 ppm, also assigned to external and internal surface silanols.

The cluster of three silanols in SSZ-70 can be more directly unveiled in a 2D ^{1}H triple-quantum (TQ)-SQ correlation experiment, Figure 2c. This spectrum clearly highlights the SiOH triad: (3.1 + 4.2 + 5.5) ppm = 12.8 ppm. The DQ autocorrelation signals at 1 to 3 and 4.2 ppm are absent in Figure 2c, proving that they are due to pairs rather than triplets. In contrast, such a TQ-SQ correlation experiment taken on ITQ-1 yields no signal (not shown). Therefore, the silanol triads found in SSZ-70 are absent in ITQ-1.

The experimental finding that the three silanol groups in the nest yield distinct chemical shifts is further addressed via electronic-structure calculations. We considered two structural motifs in DFT cluster calculations: a) a cyclic and b) an

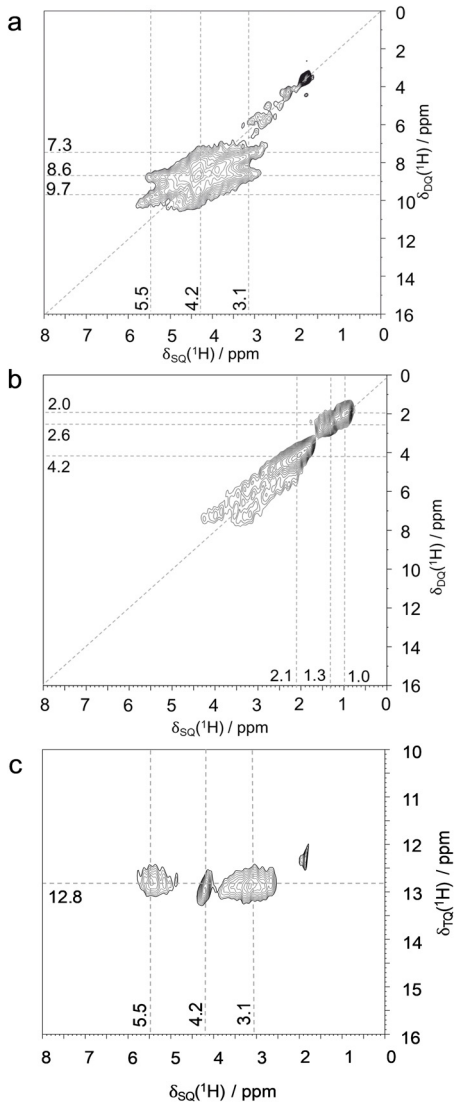

Figure 2. 2D ^{1}H DQ-SQ MAS NMR spectra of calcined a) all-silica zeolite SSZ-70, b) ITQ-1, c) 2D ^{1}H TQ-SQ MAS NMR spectrum of all-silica SSZ-70.

open triad with one OH-bond bridging another Si-O-Si oxygen atom across an adjacent 5-ring. The optimized structures are reported in Figure 3. The cyclic triad, Figure 3a, retains a distorted, cyclic silanol structure, with hydrogen-bond lengths of 1.70–1.80 Å (O···H) and O···O distances of 2.62–2.68 Å. The acyclic structure, Figure 3b, is distorted to a greater extent. The hydrogen bond formed between the external SiOH group (O2b″) and an Si-O-Si bridge (O7″) is significantly longer (d(H···O) = 2.35 Å) than the internal ones (d(H···O) = 1.63, 1.69 Å), the internal ones on the other hand are shorter than in the cyclic structure. The calculated chemical shifts of the acyclic model of Figure 3b are 3.10, 7.46, and 8.60 ppm. The span of these chemical shifts considerably exceeds the experimental ones. In terms of energy, this open silanol triad is 5.8 kcal mol^{-1} less stable than the cyclic form. Notably, the chemical shifts of the cyclic cluster model are not equivalent (6.35, 7.17, 7.68 ppm), and their span agrees much better with the experimental values.

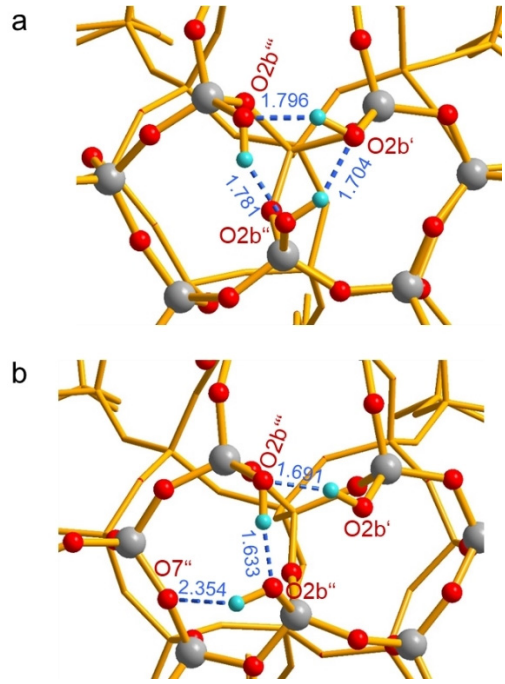

Figure 3. DFT-optimized structures (PBE-D3/def2-SVP) of two cluster models of the silanol triad in SSZ-70, a) cyclic, b) open triad; cyan H, red O, gray Si. Bond lengths in [Å]. Full cluster models with all 65 T atoms are shown in the Supporting Information.

Therefore, we propose that the triad nests in SSZ-70 are best described by a cyclic model, although the DFT calculations overestimate the strengths of the hydrogen bonds. However, some contribution of the acyclic model possibly in equilibrium with the cyclic structure appears to be feasible.

The inequivalence of the three Q^3 groups of the triad was previously observed by ^{29}Si NMR spectroscopy.[12] To explain this distortion of the crystallographic trigonal symmetry at the defect sites, the atomic occupancies of silanol monads and triads (Figure 1c) are considered. A mixture of the two models breaks the trigonal symmetry in the layer (Figure S5), and this effect is suggested to be the reason that the three silanols in the nests become inequivalent. The resolution of the coupling pattern in Figure 2a,c suggests that the monad/triad distribution follows some order within the layer. Interestingly, Berkson et al. recently reported some ordering of Al in Al-SSZ-70.[16] This suggests that such ordering is a result of charge ordering occurring during the synthesis under the influence of the structure directing agent (SDA).

The rationale for the formation of the SiOH triad in SSZ-70 is that the all-silica material needs to accommodate negative charge in order to balance the *N*,*N*′-diisobutyl imidazolium cation that is used as SDA in the synthesis of the material.[17] The defect sites in as-synthesized all-silica zeolites are well known to consist of SiOH$\cdots^{-}$OSi hydrogen bonds.[10,18] Either two or three SiOH donors interact with a charged siloxy ($^{-}$OSi) acceptor, and the ^{1}H chemical shifts in such hydrogen bonds are typically at around 10 ppm (Figure S6). The DQ-SQ data of as-synthesized Si-SSZ-70 (Figure S6) clearly reveal an autocorrelation signal ($10.3+10.3=20.6$ ppm), but a TQ-SQ autocorrelation signal is absent (near $10+10+10=30$ ppm, data not shown). It thus follows that there are two silanols in a nest for the as-synthesized material. The interaction of the SDA with the defect sites can be clearly identified here by ^{1}H DQ-SQ MAS NMR (Figure S6).

This $2\,\mathrm{SiOH}+\mathrm{SiO}^{-}$ cluster is converted into the SiOH triad in the calcined material (see above), where the SDA cation is absent and a negative charge is no longer needed. The different chemical shifts of silanol groups in the as-synthesized and calcined materials are due to the different hydrogen bond acceptor properties, that is a siloxy group, SiO^{-}, in the as-synthesized and a silanol group (or Si-O-Si moiety) in the calcined materials. It should be noted that the stability of a SiOH triad (Figure 1c), is not expected, and silanol condensation may, in general, take place upon calcination.[5b,6e] However, the SiOH triad is located in a special position in SSZ-70, where condensation of any two of the silanols would inevitably form a 3-ring. Such 3-rings are unknown in all-silica zeolites, which is obviously due to the high ring strain.

These results on SSZ-70 are in clear contrast to ITQ-1, which does not have SiOH triads upon calcination. The defects with negative framework charge in as-synthesized ITQ-1, indicated by a ^{1}H line at 10 ppm for the hydrogen bonds (Figure S6b), are instead converted into a distinct defect site structure, which shows only pairs of silanols at chemical shifts lower than for SSZ-70. This is striking, as the defect Q^3 sites in as-made all-silica zeolites often occur in a ratio of 4:1 with respect to the charge of the SDA (three SiOH hydrogen-bonded to one $^{-}$O-Si yields four Q^3 sites per charge).[17] This observation is explained by a condensation of a considerable portion of the defect silanols in ITQ-1 upon calcination, and then the material has silanols with no hydrogen bonding in a nest.

The variety of defect sites was further explored by extracting boron from B-SSZ-70. It is evident that sharp ^{29}Si MAS NMR signals are found in the all-silica material (Figure S1a), reflecting the highly ordered silanol location. In contrast, deboronated B-SSZ-70 shows much broader resonances, Figure S1b. This indicates that boron is located at different positions in the framework (see ^{11}B MAS NMR in Figure S2a), and results in a disordered location of defect sites upon boron removal. ^{1}H DQ-SQ data of B-SSZ-70 (Figure S7a) and of the deboronated material, deB-B-SSZ-70 (Figure S7b) reveal that the situation is in clear contrast to all-silica SSZ-70. The silanol triad, as found for all-silica SSZ-70, is absent in deB-B-SSZ-70. This finding is easily explained by the negative charge of $\mathrm{BO}_{4/2}^{-}$ in B-SSZ-70, making silanol nests to accommodate negative charge redundant. The deboronated material reveals silanol pairs (dyads) by a cross-correlation signal in the ^{1}H DQ-SQ correlation experiment (Figure S4b). Notably, more than two silanols cannot be confirmed (no triads or tetrads), because a TQ-SQ correlation signal is absent (Figure S7c). We conclude that removal of boron by acid leaching must lead to silanol condensation and transformation of the SiOH tetrads to a defect cluster with only two silanols. These results confirm the doubts that were raised by Senderov et al. as to the stability of a nest with four silanol groups.[6e]

We further measured FTIR spectra corresponding to Si-SSZ-70, deboronated B-SSZ-70, ITQ-1, and Aerosil 200 (amorphous silica), after pretreating each material at 250 °C and subsequently cooling down to room temperature under vacuum. The data in the Figure S1 show the O-H stretching vibration region of the infrared spectrum. On one extreme, we observe dehydroxylated Aerosil 200 (dehydroxylated at 500 °C) to exhibit a narrow band at 3740 cm^{-1}, which is known to be representative of isolated terminal silanols. Silanols that are hydrogen bonded will generally tend to exhibit a lower frequency O-H stretching vibration,[19] and all crystalline materials contain such hydrogen-bonded silanols. The material with the highest intensity of low energy bands in this region is Si-SSZ-70. This is consistent with Si-SSZ-70 being the only material with a silanol triad. To assess differences in acid strength, we adsorbed pyridine and followed its desorption under vacuum at various temperatures via FTIR spectroscopy on calcined SSZ-70, deB-B-SSZ-70, ITQ-1, and amorphous silica. In all materials, the same two infrared bands (1596 cm^{-1} and 1445 cm^{-1}) were observed for hydrogen-bonded pyridine (no pyridinium cation).[20] Compared with amorphous silica, deB-B-SSZ-70, and ITQ-1, which all released 90 % or more of adsorbed pyridine at 373 K, SSZ-70 was unique in terms of its ability to retain a significant fraction—more than 30 %—of adsorbed pyridine at the same temperature. This higher affinity of pyridine to SSZ-70 is consistent with the expected greater acidity of such a silanol triad nest, and is comparable to that of hydrogen-bonded OH networks in molecules.[21]

In conclusion we have confirmed the existence of a silanol defect site nest with 3 SiOH groups in calcined zeolite SSZ-70. This defect site is negatively charged in the as-made material to balance the organic structure-directing agent. Silanol condensation is suggested to be inhibited by the high strain that would take place in the resulting 3-rings. In contrast silanol condensation is not inhibited upon calcination of all-silica ITQ-1 or boron removal from B-SSZ-70. These findings highlight that the stability and cluster size of silanol nests depends on their local framework environment, and silanol triads or tetrads are not expected to be stable in general for other zeolites.

Acknowledgements

This work was funded by the Deutsche Forschungsgemeinschaft (DFG, German Research Foundation)—KO 1817/3-1.

Conflict of interest

The authors declare no conflict of interest.

Keywords: defects · heterogeneous catalysis · silanols · solid-state NMR spectroscopy · zeolites

[1] a) J. Čejka, A. Corma, S. Zones, *Zeolites and Catalysis*, Wiley-VCH, Weinheim, **2010**; b) W. O. Haag, in *Stud. Surf. Sci. Catal. (Zeolites and Related Microporous Materials: State of the Art 1994)*, *Vol. 84* (Eds.: J. Weitkamp, H. G. Karge, H. Pfeifer, W. Hölderich), Elsevier Science B. V., Amsterdam, **1994**, pp. 1375 – 1394; c) M. Moliner, C. Martinez, A. Corma, *Angew. Chem. Int. Ed.* **2015**, *54*, 3560 – 3579; *Angew. Chem.* **2015**, *127*, 3630 – 3649; d) J. A. Rabo, G. J. Gajda, *Catal. Rev. Sci. Eng.* **1989**, *31*, 385 – 430; e) M. Stöcker, *Microporous Mesoporous Mater.* **2005**, *82*, 257 – 292; f) S. P. Bates, R. A. van Santen, *Adv. Catal.* **1998**, *42*, 1 – 114.

[2] a) R. Gläser, J. Weitkamp, in *Handbook of Porous Solids*, *Vol. 1* (Eds.: F. Schüth, K. S. W. Sing, J. Weitkamp), Wiley-VCH, Weinheim, **2002**; b) E. E. Mallon, M. Y. Jeon, M. Navarro, A. Bhan, M. Tsapatsis, *Langmuir* **2013**, *29*, 6546 – 6555; c) T. Karbowiak, M. A. Saada, S. Rigolet, A. Ballandras, G. Weber, I. Bezverkhyy, M. Soulard, J. Patarin, J. P. Bellat, *Phys. Chem. Chem. Phys.* **2010**, *12*, 11454 – 11466; d) D. T. Bregante, A. M. Johnson, A. Y. Patel, E. Z. Ayla, M. J. Cordon, B. C. Bukowski, J. Greeley, R. Gounder, D. W. Flaherty, *J. Am. Chem. Soc.* **2019**, *141*, 7302 – 7319.

[3] a) G. P. Heitmann, G. Dahlhoff, W. F. Hölderich, *J. Catal.* **1999**, *186*, 12 – 19; b) T. Yashima, K. Miura, T. Komatsu, *Stud. Surf. Sci. Catal.* **1994**, *84*, 1897 – 1904; c) V. R. R. Marthala, J. Frey, M. Hunger, *Catal. Lett.* **2010**, *135*, 91 – 97; d) G. P. Heitmann, G. Dahlhoff, W. F. Hölderich, *Appl. Catal. A* **1999**, *185*, 99 – 108.

[4] C. B. Khouw, M. E. Davis, *J. Catal.* **1995**, *151*, 77 – 86.

[5] a) N. A. Grosso-Giordano, A. S. Hoffman, A. Boubnov, D. W. Small, S. R. Bare, S. I. Zones, A. Katz, *J. Am. Chem. Soc.* **2019**, *141*, 7090 – 7106; b) N. A. Grosso-Giordano, C. Schroeder, A. Okrut, A. Solovyoy, C. Schöttle, W. Chassé, N. Marinkoyic, H. Koller, S. I. Zones, A. Katz, *J. Am. Chem. Soc.* **2018**, *140*, 4956 – 4960.

[6] a) A. W. Chester, Y. F. Chu, R. M. Dessau, G. T. Kerr, C. T. Kresge, *J. Chem. Soc. Chem. Commun.* **1985**, 289 – 290; b) R. M. Dessau, K. D. Schmitt, G. T. Kerr, G. L. Woolery, L. B. Alemany, *J. Catal.* **1987**, *104*, 484 – 489; c) B. Kraushaar, J. W. De Haan, J. H. C. Van Hooff, *J. Catal.* **1988**, *109*, 470 – 471; d) B. Kraushaar, L. J. M. Van De Ven, J. W. De Haan, J. H. C. Van Hooff, in *Stud. Surf. Sci. Catal.*, *Vol. 37* (Eds.: P. J. Grobet, W. J. Mortier, E. F. Vansant, G. Schulz-Ekloff), Elsevier, Amsterdam, **1988**, pp. 167 – 174; e) E. Senderov, I. Halasz, D. H. Olson, *Microporous Mesoporous Mater.* **2014**, *186*, 94 – 100; f) M. C. Silaghi, C. Chizallet, J. Sauer, P. Raybaud, *J. Catal.* **2016**, *339*, 242 – 255; g) T. Li, F. Krumeich, J. Ihli, Z. Q. Ma, T. Ishikawa, A. B. Pinar, J. A. van Bokhoven, *Chem. Commun.* **2019**, *55*, 482 – 485.

[7] a) R. A. Beyerlein, C. ChoiFeng, J. B. Hall, B. J. Huggins, G. J. Ray, *Top. Catal.* **1997**, *4*, 27 – 42; b) T. Ikeda, S. Inagaki, T. Hanaoka, Y. Kubota, *J. Phys. Chem. C* **2010**, *114*, 19641 – 19648.

[8] I. Halasz, E. Senderov, D. H. Olson, J. J. Liang, *J. Phys. Chem. C* **2015**, *119*, 8619 – 8625.

[9] a) M. Feike, D. E. Demco, R. Graf, J. Gottwald, S. Hafner, H. W. Spiess, *J. Magn. Reson. Ser. A* **1996**, *122*, 214 – 221; b) I. Schnell, H. W. Spiess, *J. Magn. Reson.* **2001**, *151*, 153 – 227.

[10] a) D. F. Shantz, J. Schmedt auf der Günne, H. Koller, R. F. Lobo, *J. Am. Chem. Soc.* **2000**, *122*, 6659 – 6663; b) G. Brunklaus, H. Koller, S. I. Zones, *Angew. Chem. Int. Ed.* **2016**, *55*, 14459 – 14463; *Angew. Chem.* **2016**, *128*, 14675 – 14679.

[11] C. Schroeder, M. R. Hansen, H. Koller, *Angew. Chem. Int. Ed.* **2018**, *57*, 14281 – 14285; *Angew. Chem.* **2018**, *130*, 14477 – 14481.

[12] S. Smeets, Z. J. Berkson, D. Xie, S. I. Zones, W. Wan, X. D. Zou, M. F. Hsieh, B. F. Chmelka, L. B. McCusker, C. Baerlocher, *J. Am. Chem. Soc.* **2017**, *139*, 16803 – 16812.

[13] C. Baerlocher, L. B. McCusker Database of Zeolite Structures. http://www.iza-structure.org/databases/ (last accessed January 2020).

[14] M. A. Camblor, A. Corma, M. J. Diaz-Cabanas, C. Baerlocher, *J. Phys. Chem. B* **1998**, *102*, 44 – 51.

[15] R. H. Archer, J. R. Carpenter, S. J. Hwang, A. W. Burton, C. Y. Chen, S. I. Zones, M. E. Davis, *Chem. Mater.* **2010**, *22*, 2563 – 2572.
[16] Z. J. Berkson, M. F. Hsieh, S. Smeets, D. Gajan, A. Lund, A. Lesage, D. Xie, S. I. Zones, L. B. McCusker, C. Baerlocher, B. F. Chmelka, *Angew. Chem. Int. Ed.* **2019**, *58*, 6255 – 6259; *Angew. Chem.* **2019**, *131*, 6321 – 6325.
[17] H. Koller, R. F. Lobo, S. L. Burkett, M. E. Davis, *J. Phys. Chem.* **1995**, *99*, 12588 – 12596.
[18] E. Dib, J. Grand, S. Mintova, C. Fernandez, *Chem. Mater.* **2015**, *27*, 7577 – 7579.
[19] R. S. McDonald, *J. Phys. Chem.* **1958**, *62*, 1168 – 1178.
[20] a) M. M. Maronna, E. C. Kruissink, R. F. Parton, F. Soulimani, B. M. Weckhuysen, W. F. Hoelderich, *Phys. Chem. Chem. Phys.* **2016**, *18*, 22636 – 22646; b) E. P. Parry, *J. Catal.* **1963**, *2*, 371 – 379.
[21] K. Araki, K. Iwamoto, S. Shinkai, T. Matsuda, *Bull. Chem. Soc. Jpn.* **1990**, *63*, 3480 – 3485.

Manuscript received: January 27, 2020
Accepted manuscript online: March 18, 2020
Version of record online: April 23, 2020

